Accepted Article

WILEY-VCH

RESEARCH ARTICLE

Novel strategy for synthesis of ultra-stable single-site Mo-ZSM-5 zeolite nanocrystals

Stanislav V. Konnov,[a†] Florent Dubray,[a†] Edwin B. Clatworthy,[a] Cassandre Kouvatas,[a] Jean-Pierre Gilson,[a] Jean-Pierre Dath,[b] Delphine Minoux,[b] Cindy Aquino,[b] Valentin Valtchev,[a] Simona Moldovan,[c] Siddardha Koneti,[c] Nikolai Nesterenko,[b] Svetlana Mintova[*,a]

[a]   Dr. Stanislav V. Konnov, Florent Dubray, Dr. Edwin B. Clatworthy, Dr. Cassandre Kouvatas, Prof. Jean-Pierre Gilson, Prof. Valentin Valtchev, Dr. Svetlana Mintova
        Normandie Université, ENSICAEN, UNICAEN, CNRS
        Laboratoire Catalyse et Spectrochimie (LCS)
        14050 Caen, France
        E-mail: svetlana.mintova@ensicaen.fr
[b]   Prof. Jean-Pierre Dath, Dr. Delphine Minoux, Dr. Cindy Aquino, Dr. Nikolai Nesterenko
        Total Research and Technologies Feluy (TRTF)
        B-7181 Seneffe, Belgium
[c]   Dr. Simona Moldovan, Dr. Siddardha Koneti
        Institut des Sciences Appliquées de Rouen, Rouen University
        Groupe de Physique des Matériaux (GPM)
        76801 Rouen, France

[†]   These authors contributed equally to this work

        Supporting information for this article is given via a link at the end of the document.

Abstract: The current energy transition presents many technological challenges, such as the development of highly stable catalysts. Herein, we report a novel "top-down" synthesis approach for preparation of a single-site Mo-containing nanosized ZSM-5 zeolite possessing atomically dispersed framework-molybdenum homogenously distributed through the zeolite crystals. The introduction of Mo heals most of the native point defects in the zeolite structure resulting in an extremely stable material. The important features of this single-site Mo-containing ZSM-5 zeolite are provided by an in-depth spectroscopic and microscopic analysis. The material demonstrates superior thermal (up to 1000 °C), hydrothermal (steaming), and catalytic (converting methane to hydrogen and higher hydrocarbons) stability, maintaining the atomically disperse Mo, structural integrity of the zeolite, and preventing the formation of silanols.

Introduction

As the world undergoes a decades-long transformation of the energy industry to low or zero carbon-based resources and fuels, natural gas (mainly CH_4) and biomass will play increasingly important roles in transitioning away from traditional fossil fuel feedstocks such as coal, light and heavy oils.[1] The shift in focus to other energy sources will require the modification of existing and the development of emerging industrial processes. Zeolites, already a key player in catalysis and separations in oil refining and petrochemistry[1a] are poised to play an important role in such technologies if the stability of metal sites in zeolite-based catalysts can be insured.[2] Moreover, dedicated crude-to-chemicals technologies will start to boost the production of chemicals from oil at refineries from ≈ 10–15% at present to ≈ 30–80% in the coming decades and many traditional facilities are already considering changing their product slate from transportation fuels to chemical feedstocks.[3]

Such scenarios would benefit from the development of novel and stable metal-containing zeolite catalysts.

For example, the dehydrogenation of propane to propylene employs alumina-supported catalysts,[4] however, state of the art synthetic procedures have demonstrated several new strategies to improve the activity and stability of zeolite-supported catalysts such as the encapsulation of metal atoms and clusters during the zeolite synthesis,[5] stabilisation of the metal phase in the zeolite channels by alkali metals,[2] and the use of framework-metal sites to stabilise extra-framework active sites.[6] Similar to the dehydrogenation of propane, there are no commercial zeolite-based catalysts for the non-oxidative conversion of methane to hydrogen and industrially important chemicals (olefins, aromatics). This process is a direct route to decarbonize methane to petrochemicals while co-producing a clean energy vector - hydrogen. A big competitive advantage relative to the other routes to produce hydrogen from methane (e.g. steam reforming process) is in no direct CO_2 emission and, as a consequence, no requirement for CO_2 capture. The route is also more carbon efficient and requires lower capital investments relative to syngas routes, which are the only industrial processes currently available to transform methane to petrochemicals. This reaction faces two critical issues: (1) low conversion due to unfavorable thermodynamics and (2) catalyst deactivation due to coke deposition at high temperatures (> 700 °C) causing irreversible damage to the zeolite structure. Recent studies on metal-containing zeolites for the non-oxidative conversion of methane, such as Mo-impregnated ZSM-5, have focussed on the optimization of the metal loading, reaction process, and catalyst regeneration.[7]

For this process to be industrially viable, the catalysts envisioned will have to possess, among other features, a low density of similar active sites (single sites), short diffusion path lengths of guest molecules (nanosized crystalline domains) to minimize secondary reactions (e.g. coking), shape selectivity (selective production of high-value aromatics such as p-xylene)

and superior hydrothermal stability. It is clear that such catalysts will have to operate outside the current "comfort zone" of conventional industrial catalytic processes. At present, metal-containing zeolites operating at high temperature in the presence of steam suffer from irreversible damages including: (1) the loss of dispersion of the metal phase, (2) structural collapse, (3) strong dealumination due to the reaction between volatile metals and framework Al, and (4) hydrolysis of Al–O–Si bonds. Such challenges are seldom addressed in the current literature. Thermal and hydrothermal stability of zeolites and the currently available methodologies for their stabilization remain important issues for the industrial scale application of novel materials or even known zeolite catalysts. In addition to the recent examples for propane dehydrogenation mentioned earlier, reported methods for the stabilization of zeolites include the addition of phosphorous in MFI,[8] ion-exchange with rare-earth metals in FAU,[9] dealumination/silication by $(NH_4)_2SiF_6$ treatments and/or partial dealumination combined with extraction of Al extra-framework species (USY).[10] Most of these stabilization strategies of zeolites are based on defect healing, or the creation of substantially "defect free" structures. Very recently, Iyoki *et al.* demonstrated the stabilization of high-silica zeolites (SiO_2/Al_2O_3 > 240, BEA, MFI and MOR type) using a liquid-mediated treatment consisting of hydroxide anions, fluoride anions and organic structure directing cations, without requiring the addition of silylating agents. The treated zeolites were able to withstand high temperature steaming conditions of 900–1150 °C.[11]

In this work we report for the first time the "top-down" synthesis of novel single-site Mo-containing ZSM-5 nanozeolite with superior stability (up to 1000 °C) by treatment of calcined nanosized zeolite with sodium molybdate under autogenous pressure. Mo is atomically dispersed in the framework of an aluminium containing MFI zeolite ([Mo]-ZSM-5) and homogeneously distributed through the crystals. Mo effectively heals silanol defects and the resulting catalyst demonstrates stable activity over consecutive catalytic reactions. The exceptional stability and performance of the single-site Mo-containing nanozeolite for H_2 and higher hydrocarbons production from CH_4 under methane dehydroaromatization (MDA) conditions was demonstrated. The single-site Mo-containing ZSM-5 nanozeolite is stable under oxidative, reductive, and steaming conditions.

Results and Discussion

1. Synthesis and comprehensive characterization of Mo-containing zeolites

The single-site [Mo]-ZSM-5 zeolite sample was synthesized following the novel procedure outlined in the experimental section and presented in Scheme S1. The synthesis approach is based on the treatment of calcined Mo-free ZSM-5 nanosized zeolite with sodium molybdate at 90 °C for 5 days under autogenous pressure, followed by purification and calcination (550 °C for 6 h). The prepared [Mo]-ZSM-5 contains 0.5 wt.% of Mo according to EDS-TEM and ICP analyses. The reference sample, R-ZSM-5, was prepared by incipient wetness impregnation of the parent Mo-free ZSM-5 nanozeolite with 1 wt.% of Mo according to standard procedures reported in the MDA literature.[12] In contrast to the direct synthesis approach

reported earlier by our group,[13] the current method allows stabilization of single metal species in already synthesized aluminium containing MFI type (ZSM-5) zeolites (Scheme S1). This new procedure can be applied to any calcined pure silica and aluminosilicate zeolites including commercially available materials.

The structural properties of the novel single-site [Mo]-ZSM-5 zeolite sample were characterized by in-depth diffraction and spectroscopic analyses. The XRD patterns of the single-site [Mo]-ZSM-5 and reference R-ZSM-5 zeolite samples are depicted in Figure 1A. The [Mo]-ZSM-5 sample is monoclinic (*P*21/*n*) while the R-ZSM-5 is orthorhombic (*Pnma*). Pristine untreated calcined Mo-free ZSM-5 was orthorhombic and the XRD pattern is provided in Figure S1 for comparison. In addition, orthorhombic symmetry was maintained for the pristine ZSM-5 that was subjected to the same treatment as that used for the preparation of the [Mo]-ZSM-5 sample, however, without the presence of sodium molybdate (Figure S1). The characteristic splitting of the diffraction peaks at 23.3, 23.8, and 24.5° 2θ in the XRD pattern of the single-site [Mo]-ZSM-5 zeolite sample is
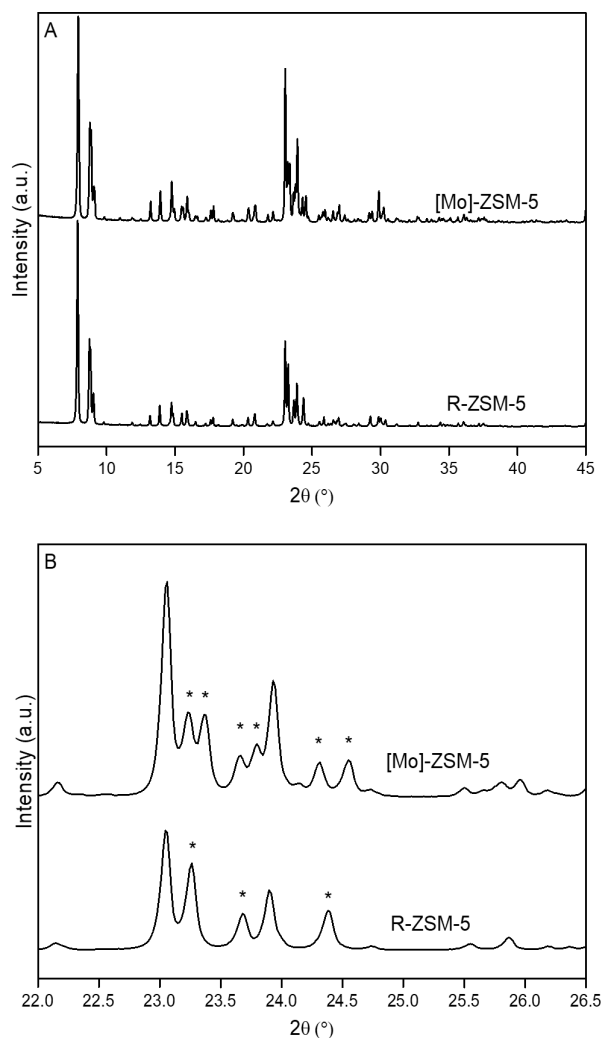

Figure 1. XRD patterns of [Mo]-ZSM-5 and R-ZSM-5 zeolite samples in the range of (A) 5–45 °2θ and (B) 22–26.5 °2θ

clearly seen (Figure 1B); stars marked the splitting of the single peaks typical for orthorhombic R-ZSM-5. The monoclinic symmetry is an indication for the isomorphous substitution of a metal with an ionic radius larger than Si in the MFI framework, however, the specific T-site locations occupied by Mo in the ZSM-5 framework were not determined.[13] The Le Bail profile refinements of the XRD patterns are summarized in Table S1. The larger unit-cell volume of the single-site [Mo]-ZSM-5 zeolite sample further indicates the substitution of Si^{IV} (ionic radius: 0.26 Å) for Mo^{VI} (ionic radius: 0.59 Å) in the MFI framework.[13] The morphology, size and elemental composition of both samples [Mo]-ZSM-5 and R-ZSM-5 are studied by STEM-HAADF (Figure 2). The statistical analysis of the particle size (measured for about 200 particles) is presented as inserts in the Figure 2A and 2B. They reveal the average particles size is about 150 ($^{+}/_{-}$ 20) nm for both Mo-ZSM-5 and R-ZSM-5 samples. The most striking differences between the samples are found in the morphology of the particles. The crystals of [Mo]-ZSM-5 exhibit smooth surfaces and sharp edges, whereas in the case of R-ZSM-5 crystals, the outer surface is less regular and the inner crystals morphology is marked by the presence of mesopores (darker circular areas). The sharpness of the edges in the case of specimen [Mo]-ZSM-5 can be interpreted as a signature of its monocrystalline nature, whilst the irregular outer edges of the R-ZSM-5 crystals are associated with their polycrystallinity. The polycrystalline nature of the R-ZSM-5 crystals is also associated with the presence of an abundant number of defects (notably the mesopores), which is further

confirmed by NMR (^{1}H and ^{29}Si MAS NMR), and IR spectroscopy (see below). The atomically dispersed Mo in [Mo]-ZSM-5 (seen as light points in the micrographs) are highlighted with circles in the STEM-HAADF micrographs, and confirm the presence of homogeneously distributed Mo atoms within the zeolite crystals (Figure 2A). The size of Mo light points in STEM-HAADF micrographs is similar in the two samples, however, they differ substantially in their stability under high temperature treatment (up to 1000 ºC) and steaming. The chemical composition of the single-site [Mo]-ZSM-5 crystals is determined by ICP and confirmed by EDS-TEM. The elemental distributions in the [Mo]-ZSM-5 and R-ZSM-5 samples are shown in Figure S2. The shape and morphology of the pristine ZSM-5 was examined by STEM-EDS (Figure S3). The agglomerated crystals have irregular shapes, and a mean size of 170 nm. The crystals in the reference sample (R-ZSM-5) have a similar shape and size (Figure S2); the distribution of both Si and Al in the pristine and reference sample is homogeneous suggesting that no changes under impregnation occurred.

Further structural information of the single-site [Mo]-ZSM-5 sample is provided by ^{29}Si MAS NMR spectroscopy (Figure 3A). The spectrum of the calcined [Mo]-ZSM-5 sample reveals well-resolved Q^4 (($SiO)_4Si$) and no Q^3 (($SiO)_3Si$-OH) species, indicating an almost total absence of silanols. In comparison, the reference R-ZSM-5 sample displays unresolved Q^4 and Q^3 species, indicating the presence of silanol defects. These results are consistent with the HRTEM observations revealing the formation of [Mo]-ZSM-5 crystals with smooth surface, while the
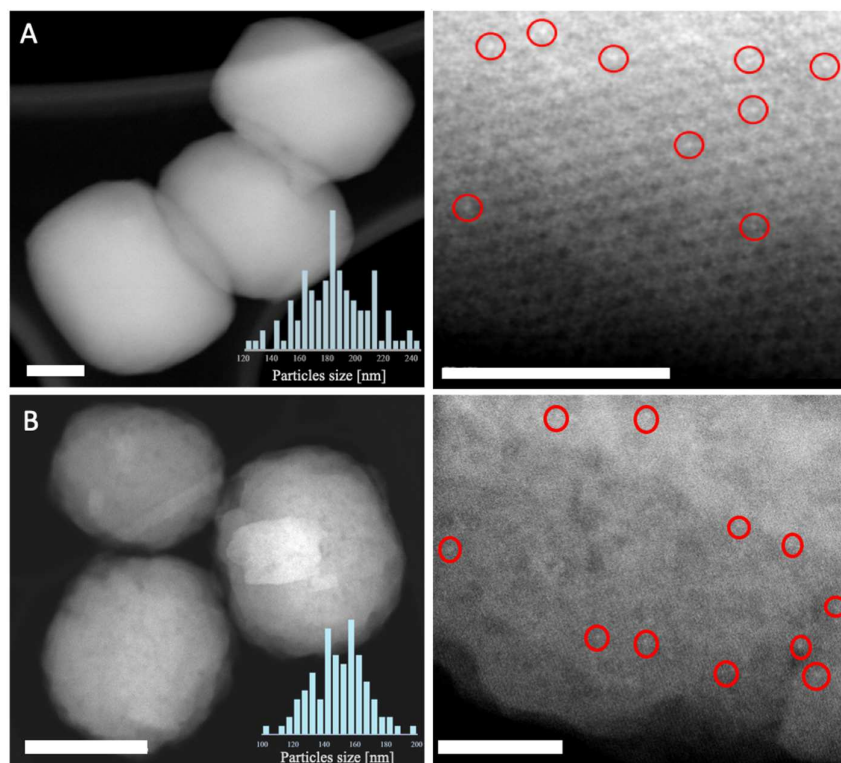

Figure 2. STEM-HAADF micrographs of (a) [Mo]-ZSM-5: left scale bar = 100 nm, right scale bar = 10 nm, and (B) R-ZSM-5: left scale bar = 100 nm, right scale bar = 10 nm. Inset: particle size distribution.

R-ZSM-5 particles contain additional mesopores and surface defects. The presence of Al in the framework of both samples is confirmed by ^{27}Al MAS NMR spectroscopy (Figure 3B). The spectra for both the [Mo]-ZSM-5 and R-ZSM-5 samples contain a sharp peak at 60 ppm corresponding to Al in tetrahedral coordination, and no octahedral species are detected at 0 ppm.

The results from the ^{29}Si and ^{27}Al NMR analyses are consistent with the IR observations performed in the silanol region for the two samples (Figure 4A). Sample [Mo]-ZSM-5 contains a negligible amount of isolated silanols represented by the peak at 3745 cm^{-1}, and no silanol nests. In comparison, sample R-ZSM-5 contains a significant amount of isolated silanols and silanol nests represented by the highly intense peaks at 3745 cm^{-1} and 3510 cm^{-1}, respectively. The peak corresponding to bridging silanol species at 3610 cm^{-1} in both samples remains unchanged, confirming the preservation of Brönsted acid sites (Figure 4A). Additionally, the low amount of silanol defects in the [Mo]-ZSM-5 is confirmed by ^{1}H MAS NMR spectroscopy (Figure 4B); the samples were dehydrated at 200 °C overnight prior to the measurements to remove the zeolitic water. One peak at 2.3 ppm corresponding to isolated silanol species is present in the spectrum of [Mo]-ZSM-5, while no peaks in the range 4–5.5 ppm are observed which is attributed to the absence of silanol nests. For the R-ZSM-5 reference sample, broad peaks at 2.3, and 4.0–5.5 ppm related to isolated silanols, and silanol nests and/or bridging hydroxyl groups respectively are observed (Figure 4B).[14]

The location and state of the Mo are further studied by ^{31}P MAS NMR spectroscopy. The spectra of adsorbed trimethylphosphine oxide (TMPO) on the single-site [Mo]-ZSM-5 and reference R-ZSM-5 samples are presented in Figure 5. The presence of Mo in the framework positions of the [Mo]-ZSM-5 zeolite is confirmed by the resonance at 45 ppm which is consistent with previous work,[13] while a small amount of silanols are also observed (50 ppm).[15] Two Brönsted acid sites (64 and 74 ppm) as well as crystalline (43 ppm) and physisorbed (29 ppm) TMPO are present, indicating that TMPO accesses all acidic and metallic sites.[15c, 16] In contrast, for the Mo impregnated R-ZSM-5 sample, Brönsted acid sites (64 and 74 ppm) and silanols (50 ppm) are present, however, no framework Mo is detected as the resonance at 45 ppm is not observed (Figure 5).
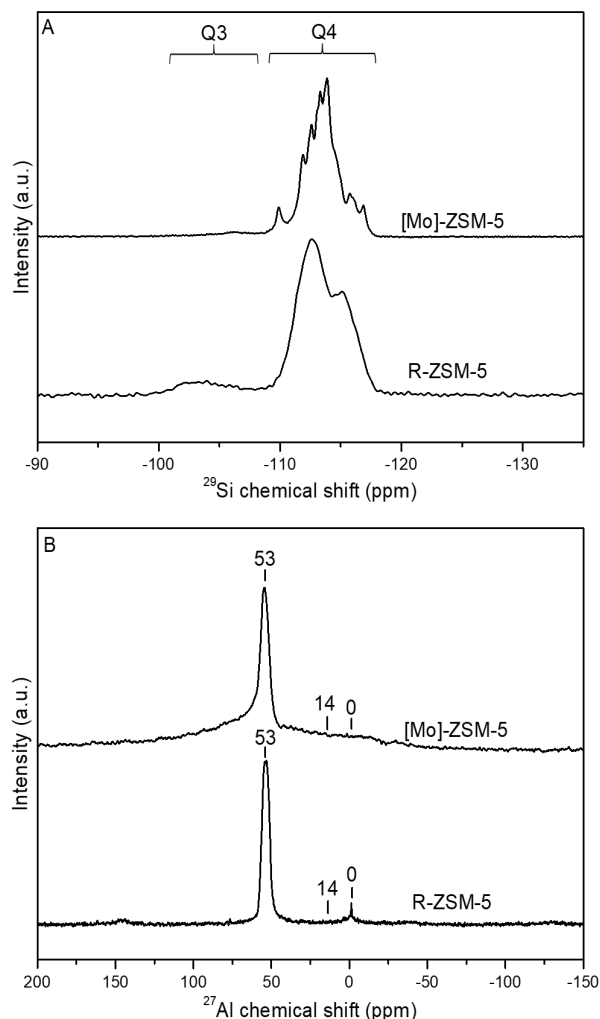

Figure 3. (A) ^{29}Si MAS NMR and (B) ^{27}Al MAS NMR spectra of samples [Mo]-ZSM-5 and R-ZSM-5.
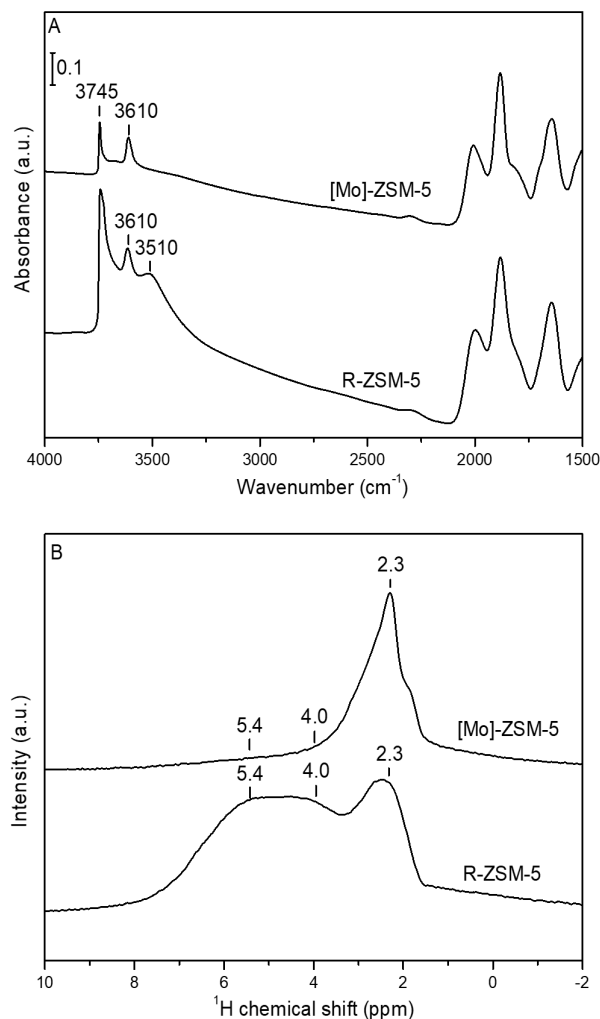

Figure 4. (A) FTIR spectra and (B) ^{1}H MAS NMR spectra of dehydrated [Mo]-ZSM-5 and R-ZSM-5 samples.
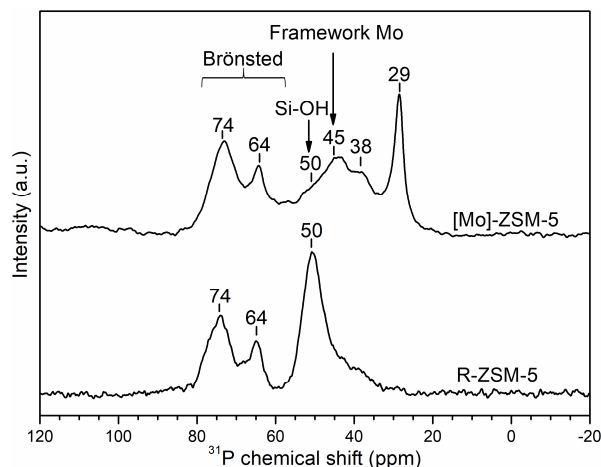
Figure 5. ^{31}P MAS NMR spectra of TMPO adsorbed on samples [Mo]-ZSM-5 and R-ZSM-5.

2. Catalytic test of Mo-containing ZSM-5 zeolite samples: non-oxidative high temperature CH4 conversion to H2 and higher hydrocarbons

The catalytic performances of the Mo single-site [Mo]-ZSM-5 and reference R-ZSM-5 samples were assessed for the high temperature non-oxidative conversion of CH_4 (850 °C, atmospheric pressure, 0.3 g of catalyst, WHSV 1.2 h^{-1}) over 12 h (Figure 6). The reference sample, R-ZSM-5, rapidly deactivates until the conversion of CH_4 plateaus after 7 h. In contrast, the single-site [Mo]-ZSM-5 zeolite sample with only 0.5 % Mo shows exceptional stability after three consecutive reaction-regeneration cycles. It is worth noting that for [Mo]-ZSM-5, we deal with Mo-sites which remain within the zeolite framework allowing for the presence of either non-carburized or partially carburized Mo-sites. The location and retention of Mo in the zeolite framework results in the high stability of the catalyst, allowing it to operate under severe conditions over multiple reaction-regeneration cycles. However, further in-depth study is required to determine the exact structure and evolution of the actives sites. Mo remains in the framework structure of the [Mo]-ZSM-5 zeolite and does not undergo any discernible changes over the three reaction-regeneration cycles, *vide infra*. The total methane conversion to hydrogen and the detailed product yields of the two catalysts are compared in Figure 6B. The [Mo]-ZSM-5 sample affords a significantly higher yield of hydrogen and ethylene in comparison to the R-ZSM-5 reference sample. It is also worth noting that the [Mo]-ZSM-5 sample produces a relatively high proportion of ethylene in the C_2 fraction (> 90%). The production of C_3-C_4 hydrocarbons is negligible for both samples.

To assess the stability of the Mo in the single-site [Mo]-ZSM-5 zeolite sample, the catalysts were subjected to multiple cycles of reaction (MDA, *i.e.* reducing conditions) and regeneration (calcination, *i.e.* oxidative conditions). Under typical MDA operating conditions, the classical Mo containing zeolite (R-ZSM-5) deactivates due to the sintering and migration of molybdenum carbide species as a consequence of weak interactions with the zeolite.[17] During the exothermic catalyst regeneration, the molybdenum carbide is oxidized, and steam is generated from the oxidation of coke. Under such conditions the Mo species become mobile and react with framework Al to form aluminium molybdates. These new Mo species cannot form

carbides, resulting in irreversible deactivation of the catalyst.[15a, 18] In contrast, the single-site [Mo]-ZSM-5 nanozeolite shows exceptional stability for the conversion of CH_4 after three reactions at 850 °C and regeneration cycles at 750 °C (Figure 6A). Moreover, the [Mo]-ZSM-5 catalyst produces relatively stable amounts of hydrogen and aliphatics throughout the cycles in comparison with the R-ZSM-5 sample (Figure S4). Such a stable catalytic performance of the [Mo]-ZSM-5 over three reaction-regeneration cycles clearly demonstrates that the catalytically active sites attributed to the single-site Mo in the MFI structure are maintained, in strong contrast with the reference R-ZSM-5 sample. That the catalyst demonstrates stable activity at a high reaction temperature (850 °C) allows for the targeted production of ethylene which requires more severe conditions. The [Mo]-ZSM-5 catalyst can operate over a greater temperature range without significant changes in its catalytic performance, which is one of the critical points for process design. The significant improvement in the stability of the metal
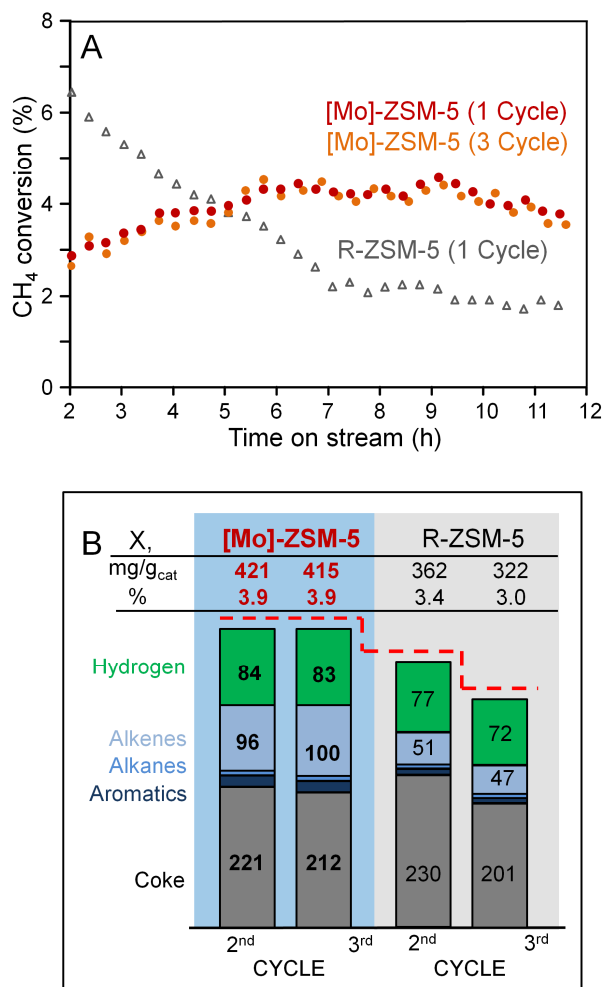

Figure 6. (A) CH_4 conversion after the first and third consecutive cycles of reaction-regeneration as a function of time on stream for the [Mo]-ZSM-5 and reference R-ZSM-5 catalysts and (B) total CH_4 conversion (X: milligrams per gram of catalyst or %), products yield (milligrams per gram of catalyst) corresponding to 2–12 h time gap of calculation over the [Mo]-ZSM-5 and R-ZSM-5. Reaction conditions: T = 850 °C, atmospheric pressure, WHSV = 1.2 h^{-1}, time on stream window = 2–12 h.

phase is highly beneficial, in particular for catalysts working under harsh conditions (*e.g.* high temperatures and continuous oxidation/reduction cycles).

As shown above, the single-site metal species incorporated into the zeolite framework results in stable catalytic performance. Further investigation of the thermal and hydrothermal stability of the single-site Mo-containing [Mo]-ZSM-5 zeolite and the reference sample is provided below. Emphasis is placed on the characterization of the samples in an attempt to describe the structural evolution of the catalysts under harsh reaction and regeneration conditions.

3. Stability and Mo-containing zeolite samples.

The stability of the single-site [Mo]-ZSM-5 and the reference [R]-ZSM-5 zeolite samples was evaluated after the catalytic reaction and subsequent recycling treatments. The samples subjected to 3 catalytic (reaction-regeneration) cycles are denoted with "(3 cycles)", while the samples that are subjected to 3 catalytic cycles followed by steaming are denoted with "(S)". The XRD patterns of the calcined ([Mo]-ZSM-5) and used ([Mo]-ZSM-5 (3 cycles)) samples after 3 catalytic cycles (methane conversion and regeneration at 750 °C) clearly show that all the Bragg peaks are identical, confirming the preservation of the crystalline structure (Figure S5). A marginal decrease of the unit cell volume for [Mo]-ZSM-5 (3 cycles) is observed, suggesting that the sample underwent a degree of dealumination (Table S1). In contrast, the unit cell volume of R-ZSM-5 sample decreased substantially from 5359.283 to 5344.653 Å^3, which is indicative of significant structural change occurring in the sample R-ZSM-5 (3 cycles). Remarkably, the ^{29}Si MAS NMR spectrum of the single-site [Mo]-ZSM-5 (3 cycles) sample is almost identical to that of the calcined [Mo]-ZSM-5 sample (Figure S6). The ^{29}Si MAS NMR spectra of [Mo]-ZSM-5 (3 cycles) still displays highly resolved Q^4 species and no Q^3 species, in stark contrast to R-ZSM-5 (3 cycles) where both Q^3 and Q^4 species are observed. This further demonstrates the exceptional stability of the framework Mo in the [Mo]-ZSM-5 zeolite under reductive (catalytic reaction) and oxidative (regeneration) conditions. The intensity and high resolution of the Q^4 peaks in the spectrum of the [Mo]-ZSM-5 (3 cycles) sample is related to the degree of dealumination, the conservation of Mo in the structure, and the absence of silanols. The occurrence of dealumination in both the [Mo]-ZSM-5 (3 cycles) and R-ZSM-5 (3 cycles) samples was revealed in the ^{27}Al MAS NMR spectra by the presence of octahedral aluminum species at 0 ppm (Figure S7). Based on ^{27}Al MAS NMR spectroscopy, dealumination occurred to a slightly greater degree for the [Mo]-ZSM-5 (3 cycles) sample in comparison to the R-ZSM-5 (3 cycles) sample. This suggests that the Brønsted sites due to framework Al in the Mo impregnated ZSM-5 (R-ZSM-5 sample) are more resilient to dealumination than in pure ZSM-5. This discrepancy could be attributed to the presence of a protective molybdenum oxide shell around the framework Al species in the R-ZSM-5 sample consistent with recent work reporting a preferential location of Mo near framework Al species in ZSM-5.[19]

Additionally, the stability of the samples after 3 catalytic cycles was studied after a subsequent steaming treatment performed at 550 °C. The XRD patterns and ^{29}Si MAS NMR spectra of the [Mo]-ZSM-5 (S) and R-ZSM-5 (S) samples (Figure 7) establishes the outstanding hydrothermal stability of the framework Mo species in [Mo]-ZSM-5 zeolite. All the Bragg peaks are identical for the calcined [Mo]-ZSM-5 and the

steamed [Mo]-ZSM-5 (S) samples, while the diffraction pattern of the R-ZSM-5 (S) sample reveals the appearance of several Bragg peaks (Figure 7A). In addition, the ^{29}Si MAS NMR spectra of the [Mo]-ZSM-5 (S) sample (Figure 7B) displays highly resolved Q^4 species and no Q^3 species, demonstrating that no silanol species were generated after the combined reaction-regeneration cycles and steaming treatments despite the simultaneous occurrence of dealumination. These observations further support the conclusion that the Mo atoms are retained in the MFI framework. This is the first example of a zeolite structure that contains heteroelements, such as Mo, able to withstand such harsh treatment (3 high temperature reaction/regeneration cycles in MDA, followed by steaming at 550 °C). In contrast, the R-ZSM-5 (S) sample displays both unresolved Q^4 and Q^3 species attributed to the presence of silanol species. The formation of aluminium molybdates and the
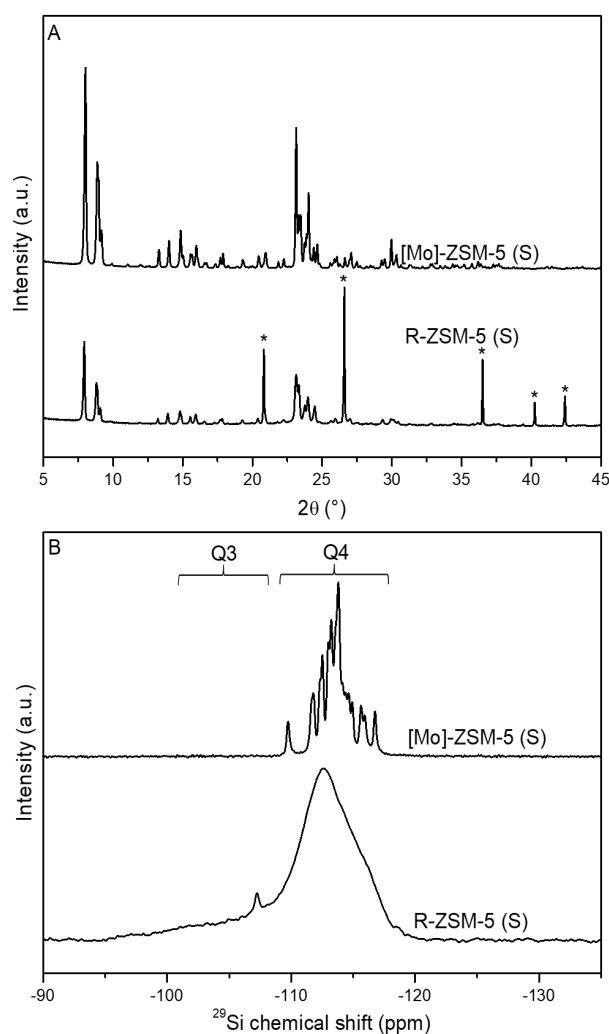

Figure 7. (A) XRD patterns, and (B) ^{29}Si MAS NMR spectra of samples [Mo]-ZSM-5 (S) and R-ZSM-5 (S). Diffraction peaks marked by "*" at 20.8, 26.6, 36.5, 40.2, and 42.4 ° 2θ on sample R-ZSM-5 (S) are attributed to the formation of catalytically inactive aluminium molybdate species.

occurrence of dealumination of the R-ZSM-5 (S) sample were further supported by ^{27}Al MAS NMR analysis (Figure 8A) due to the clear appearance of a peak at 14 ppm, which was not observed for the [Mo]-ZSM-5 (S) sample. Indeed, in the case of the [Mo]-ZSM-5 (S) sample, a portion of the tetrahedral Al (53 ppm) is converted to distorted framework Al and/or penta-coordinated Al species (27 ppm), and octahedral Al. Critically, no aluminum molybdate is formed, in stark contrast with the R-ZSM-5 (S) sample. Indeed, it has been reported that MoO_3 reacts with framework Al above 550 °C to form aluminum molybdate and possibly surface $AlMo_6$ Anderson entities.[7a] Consequently, the absence of aluminum molybdate in [Mo]-ZSM-5 (S) further indicates that all Mo atoms remain atomically dispersed in the framework of [Mo]-ZSM-5 after steam treatment. ^{31}P MAS NMR spectra (using TMPO) of the steamed samples are depicted in Figure 8B. The number of Brønsted acid sites in the [Mo]-ZSM-5 (S) sample decreased substantially after steaming due to dealumination and the subsequent formation of extra-framework aluminium, evidenced from both ^{31}P MAS NMR (Figure 8B) and ^{27}Al MAS NMR (Figure 8A) spectroscopy, *vide*

supra. Importantly, no silanols are observed after the reaction-regeneration cycles and subsequent steaming of the [Mo]-ZSM-5 sample according to the ^{31}P MAS NMR spectra (Figure 8B), even though dealumination occurs. This demonstrates that atomically dispersed Mo introduced into the MFI zeolite framework stabilizes the crystalline structure and prevents the formation of silanols. This is further supported by the fact that, despite the occurrence of dealumination, the resonance at 45 ppm remains unchanged, suggesting that Mo is retained in the framework.

Conclusion

Here we report the synthesis of a novel single-site [Mo]-ZSM-5 zeolite using a Mo-free ZSM-5 nanosized zeolite subjected to treatment with sodium molybdate under autogenous pressure. The single-site [Mo]-ZSM-5 zeolite contains highly disperse Mo (0.5 wt.%) according to EDS-TEM and ICP analyses; the Mo]-ZSM-5 zeolite was compared with a reference sample prepared with 1 wt.% Mo by the classical impregnation method (R-ZSM-5). The properties of the single-site Mo containing ZSM-5 zeolite were characterized at the atomistic and molecular level using diffraction, microscopy and spectroscopy methods.

The novel single-site Mo-containing nanozeolite possesses atomically dispersed framework-molybdenum atoms homogenously distributed through the zeolite crystals. The introduction of atomically dispersed Mo in the zeolite framework heals silanol defects resulting in an extremely stable material, resistant to severe structural degradation. The novel single-site Mo-containing ZSM-5 nanozeolite exhibits superior performance for CH_4 conversion to H_2 and higher hydrocarbons operating under successive reductive and oxidative atmospheres at high temperature (850 and 750 °C), as well as demonstrating exceptional structural stability under hydrothermal steaming conditions.

In summary, zeolites have so far been used successfully and extensively in oil refining and petrochemistry, and will continue to play an important role by meeting the challenges in these fields. However, the operating conditions (e.g. temperatures in the 750–850 °C range) of some emerging industrial processes will push zeolites outside this "comfort zone" and successful zeolitic catalysts will require exceptional thermal and hydrothermal resilience.

The single-site Mo-containing ZSM-5 represents a strong example of a zeolite material able to operate "outside" of the comfort zone. This novel synthesis approach can be applied for the introduction of other metals (e.g. V, W, Cu, Zn) in other calcined zeolites including pure silica and aluminosilicates.
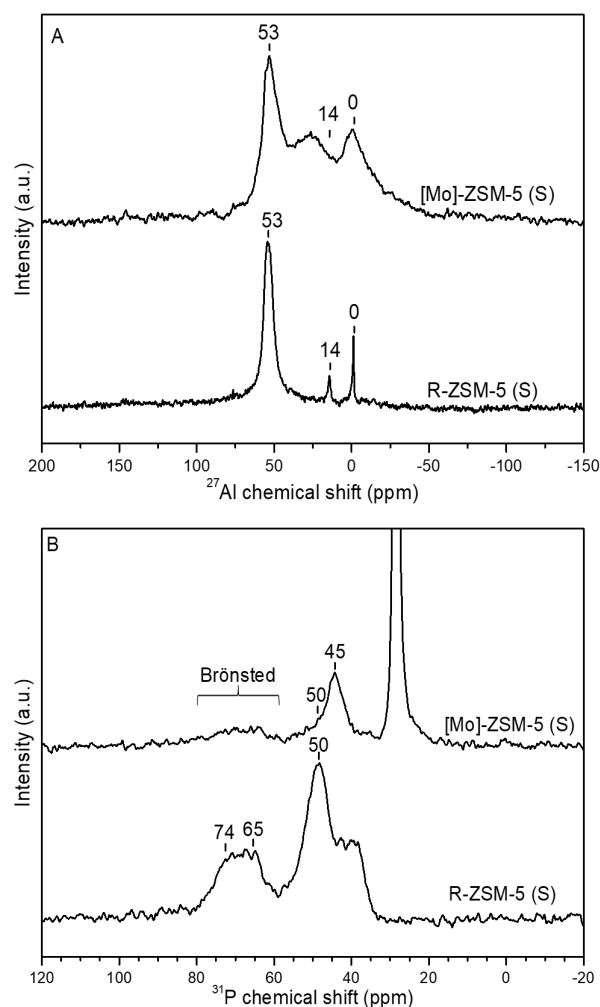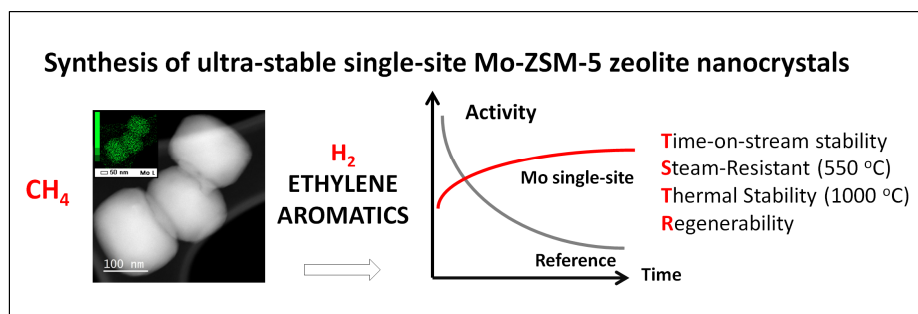

Figure 8. (A) ^{27}Al MAS NMR spectra of dehydrated [Mo]-ZSM-5 (S) and R-ZSM-5 (S) samples, and (B) ^{31}P MAS NMR spectra of TMPO adsorbed on dehydrated [Mo]-ZSM-5 (S) and R-ZSM-5 (S) samples.

Acknowledgements

10.1002/anie.202006524

[1]   a) V. Smil, *Energy and civilization: a history*, MIT Press, Cambridge, Massachusetts, **2017**; b) V. Smil, *Energy transitions: global and national perspectives*, 2nd ed., Praeger, **2016**; c) W. Vermeiren, J.-P. Gilson, *Top. Catal.* **2009**, *52*, 1131-1161.

[2]   L. Liu, M. Lopez-Haro, C. W. Lopes, C. Li, P. Concepcion, L. Simonelli, J. J. Calvino, A. Corma, *Nat. Mater.* **2019**, *18*, 866-873.

[3]   M. Chadwick, G. McManus, S. Zinger, G. Haire, *Crude-to-Chemicals: Opportunity or Threat?*, Wood Mackenzie, **2019**

[4]   J. J. Sattler, J. Ruiz-Martinez, E. Santillan-Jimenez, B. M. Weckhuysen, *Chem. Rev.* **2014**, *114*, 10613-10653.

[5]   L. Liu, U. Diaz, R. Arenal, G. Agostini, P. Concepción, A. Corma, *Nat. Mater.* **2017**, *16*, 132-138.

[6]   a) Y. Wang, Z.-P. Hu, W. Tian, L. Gao, Z. Wang, Z.-Y. Yuan, *Catal. Sci. Technol.* **2019**, *9*, 6993-7002; b) Z. Xu, Y. Yue, X. Bao, Z. Xie, H. Zhu, *ACS Catal.* **2019**, *10*, 818-828.

[7]   a) N. Kosinov, F. J. Coumans, G. Li, E. Uslamin, B. Mezari, A. S. Wijpkema, E. A. Pidko, E. J. Hensen, *J. Catal.* **2017**, *346*, 125-133; b) H. Ma, R. Kojima, R. Ohnishi, M. Ichikawa, *Appl. Catal. A* **2004**, *275*, 183-187; c) S. J. Han, S. K. Kim, A. Hwang, S. Kim, D.-Y. Hong, G. Kwak, K.-W. Jun, Y. T. Kim, *Appl. Catal. B* **2019**, *241*, 305-318.

[8]   a) T. Blasco, A. Corma, J. Martínez-Triguero, *J. Catal.* **2006**, *237*, 267-277; b) W. W. Kaeding, S. A. Butter, *J. Catal.* **1980**, *61*, 155-164; c) A. Jentys, G. Rumplmayr, J. A. Lercher, *Appl. Catal.* **1989**, *53*, 299-312; d) H. E. van der Bij, B. M. Weckhuysen, *Chem. Soc. Rev.* **2015**, *44*, 7406-7428.

[9]   J. Biswas, I. Maxwell, *Appl. Catal.* **1990**, *63*, 197-258.

[10]   A. Corma, V. Fornes, F. Rey, *Appl. Catal.* **1990**, *59*, 267-274.

[11]   K. Iyoki, K. Kikumasa, T. Onishi, Y. Yonezawa, A. Chokkalingam, Y. Yanaba, T. Matsumoto, R. Osuga, S. P. Elangovan, J. N. Kondo, *J. Am. Chem. Soc.* **2020**, *142*, 3931-3938.

[12]   D. Wang, J. H. Lunsford, M. P. Rosynek, *J. Catal.* **1997**, *169*, 347-358.

[13]   F. Dubray, S. Moldovan, C. Kouvatas, J. Grand, C. Aquino, N. Barrier, J.-P. Gilson, N. Nesterenko, D. Minoux, S. Mintova, *J. Am. Chem. Soc.* **2019**, *141*, 8689-8693.

[14]   W. Zhang, X. Bao, X. Guo, X. Wang, *Catal. Lett.* **1999**, *60*, 89-94.

[15]   a) B. Liu, J. Leung, L. Li, C. Au, A.-C. Cheung, *Chem. Phys. Lett.* **2006**, *430*, 210-214; b) J. D. Lewis, M. Ha, H. Luo, A. Faucher, V. K. Michaelis, Y. Román-Leshkov, *ACS Catal.* **2018**, *8*, 3076-3086; c) A. Zheng, S.-B. Liu, F. Deng, *Chem. Rev.* **2017**, *117*, 12475-12531.

[16]   C. Bornes, M. Sardo, Z. Lin, J. Amelse, A. Fernandes, M. F. Ribeiro, C. Geraldes, J. Rocha, L. Mafra, *Chem. Commun.* **2019**, *55*, 12635-12638.

[17]   P. Schwach, X. Pan, X. Bao, *Chem. Rev.* **2017**, *117*, 8497-8520.

[18]   C. H. Tempelman, E. J. Hensen, *Appl. Catal. B* **2015**, *176*, 731-739.

[19]   L. Liu, N. Wang, C. Zhu, X. Liu, Y. Zhu, P. Guo, L. Alfilfil, X. Dong, D. Zhang, Y. Han, *Angew. Chem.* **2020**, *132*, 829-835.

Entry for the Table of Contents

Synthesis of ultra-stable single-site Mo-ZSM-5 zeolite nanocrystals

CH$_4$

H$_2$
ETHYLENE
AROMATICS

Activity

Mo single-site

Reference

Time

Time-on-stream stability
Steam-Resistant (550 ^{o}C)
Thermal Stability (1000 ^{o}C)
Regenerability

A single-site Mo-containing nanosized ZSM-5 zeolite with atomically dispersed framework-molybdenum is synthesized. The single-site Mo-containing nanosized ZSM-5 zeolite displays superior thermal (1000 °C), hydrothermal (steaming), and catalytic (converting methane to hydrogen and higher hydrocarbons) stability, maintaining the atomically disperse Mo, structural integrity of the zeolite, and preventing the formation of silanols.

.